Improved ZVT PWM Converters Using An Auxiliary Resonant Source

M. L. S. Martins, H. L. Hey, J. R. Pinheiro, H. Pinheiro and H. A. Gründling

Power Electronics and Control Research Group - GEPOC
Federal University of Santa Maria - UFSM
97105-900 - Santa Maria - RS - Brazil
hey@ctlab.ufsm.br - www.ufsm.br/gepoc

Abstract - This paper presents a novel family of Zero Voltage Transition (ZVT) Commutation Cell for PWM DC-DC Converters that uses a resonant circuit as auxiliary commutation source to control the current through the auxiliary switch. The improved ZVT commutation cell enables the main switch to be turned on and off at Zero Voltage Switching (ZVS) and the auxiliary switch to be turned on and off at Zero Current Switching (ZCS).

To verify the feasibility of the proposed commutation cell, it is applied to a DC-DC PWM boost converter. Operation principles are in good agreement with experimental results obtained from prototype rated at 1.0 kW operating at 100 kHz.

I. INTRODUCTION

Due to the current tendency of producing electronic equipments with higher efficiency, power density and EMI performance, the search for more efficient soft switching techniques has become indispensable. Among these techniques, the commutation at zero voltage (ZVT- Zero Voltage Transition) has been frequently used due its relative simplicity, efficiency and reliability. The auxiliary commutation network of the converter is placed in parallel with the main power path, reducing its interference on the converter operation. Furthermore, assuring lower conduction losses through it, because the auxiliary commutation elements do not need to be rated for the total converter power, but rather just for a small fraction of that power.

Although ZVT is a well-accepted technique, several ZVT commutation cells proposed in the literature suffer from some drawbacks such as hard commutation and/or turn-on capacitive losses at auxiliary switching [1,2], additional components count [3], higher main switch current stresses [4,5,6,7,9], higher auxiliary switch voltage stresses [8,9] and output characteristics limitations [10]. Among the ZVT commutation cell the most attractive solution is presented in [13]. However, it needs an autotransformer in the commutation cell to perform the auxiliary commutation source.

The aim of this paper is to propose an improved ZVT commutation cell that uses a resonant tank as auxiliary commutation source that minimize main drawbacks mentioned above and in addition without needing a transformer (or auto-transformer) to perform the auxiliary commutation source.

This paper is organized as follows: Section II introduces a new family of the Improved ZVT PWM DC-DC of converters, as well as the operation principle of the improved ZVT boost converter. In Section III, the soft commutation conditions are described. In Section IV a design guideline is presented and illustrated with an example. Section V verifies the feasibility of the proposed ZVT commutation cell presenting results from a prototype rated at 1 kW operating at 100 kHz. Finally, Section VI draws some conclusions from the analysis of the experimental results obtained.

II. PRINCIPLES OF OPERATION OF THE IMPROVED ZVT BOOST CONVERTER

A. Improved ZVT Converter with Resonant Auxiliary Circuit.

A new class of soft-switching converter was proposed in [1], namely ZVT PWM converters. These converters use a few additional elements placed in a parallel path with the main power circuit providing zero voltage commutation for the main switch without additional voltage and current stresses. Thus, this approach overcame the main drawbacks presented in the ZVS-QRC converters [11] and ZVS-PWM converters [12]. However, in [1] the auxiliary switch commutates hard, reducing the overall efficiency gain and the EMI performance. To overcome these drawbacks this paper proposes an improved ZVT commutation cell shown in Fig. 1. It maintains the merits present in [1] and furthermore, achieving soft switching at zero current (ZCS) for auxiliary switch. To obtain these characteristics a resonant tank, which plays the role of the auxiliary source, is used to control the current through the auxiliary switch. This resonant tank is represented by the inductor L_{r1} and the capacitor C_r.

Fig. 2 shows a family of improved ZVT PWM DC-DC non-isolated converters obtained by incorporating the auxiliary resonant commutation cell. They are based on the common equivalent circuit of DC-DC converters presented in [14]. It can be seen that the auxiliary commutation cell is placed in parallel with the main power path. The terminal "d" of the commutation cell can be connected either with the terminal "y" or with the terminal "z".

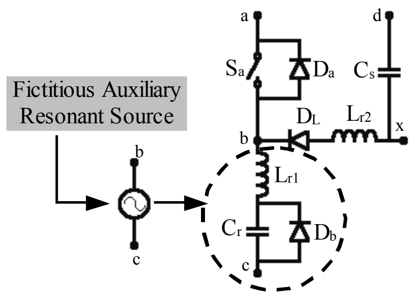

Fig. 1 – Improved ZVT Auxiliary Commutation Cell.

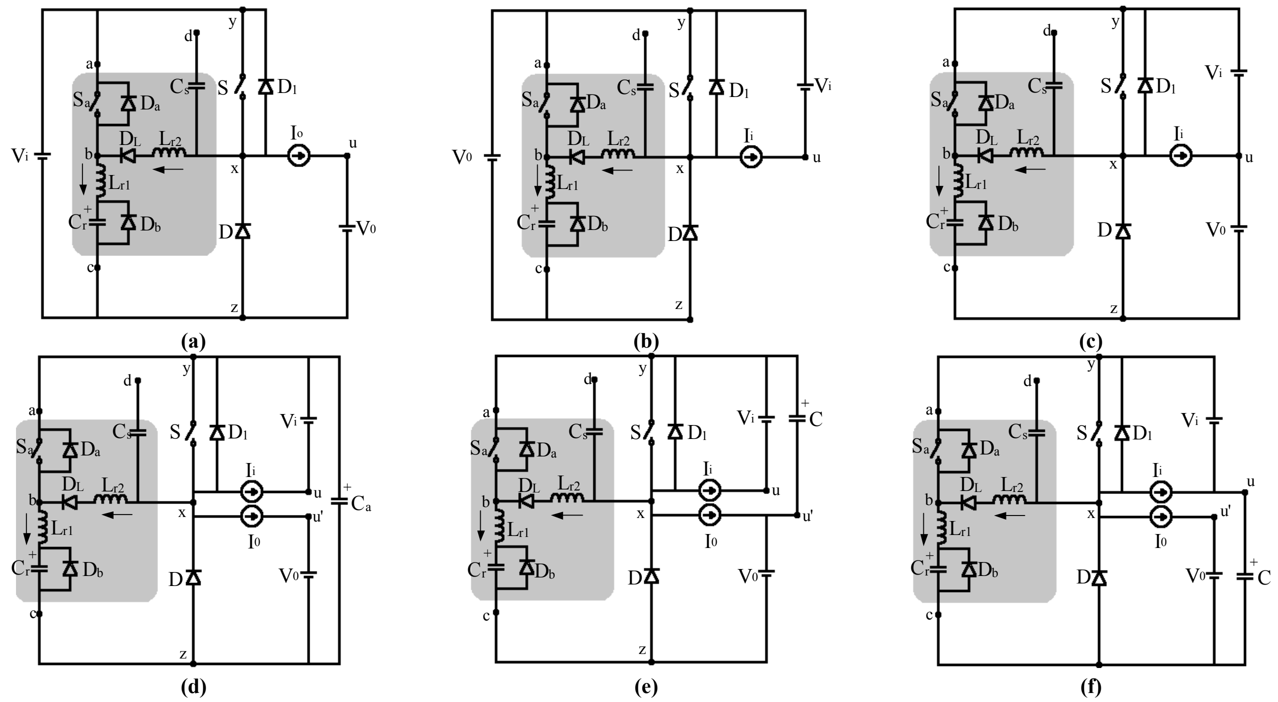

Fig. 2 – The Improved ZVT Family Converters.
(a) Buck; (b) Boost; (c) Buck-boost; (d) Cúk; (e) Sepic; (f) Zeta.

B. Operation Principles

To analyze the operation of the proposed improved ZVT DC-DC PWM converters, the improved ZVT PWM boost converter was chosen. Fig. 3 shows the improved ZVT PWM boost converter represented in the conventional topological form. It differs from the boost converter presented in Fig. 2(b) just by the components placement. The steady-state analysis of this boost converter is carried out using the following assumptions:

i) the input inductor is large enough to be considered as a constant current source I_i during one switching period;
ii) the output capacitor is large enough to be considered as a constant voltage source V_0;
iii) all the semiconductors are considered ideals.

In the steady state operation this converter assumes nine different circuit modes in one switching period as shown in Fig. 5. The description of each circuit mode is presented as follow. Before the instant t_0 the diode D is conducting the input current I_i. The voltages across both switches are equal to the output converter voltage V_0 and voltage across auxiliary capacitor C_r is zero. The main theoretical waveforms are presented in Fig. 4.

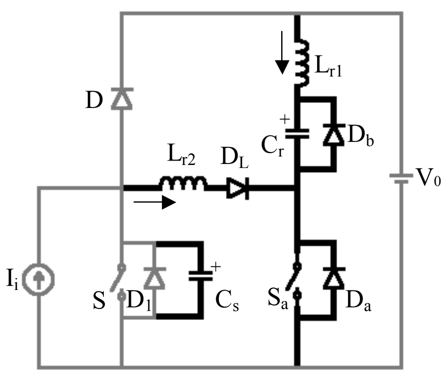

Fig. 3 – Improved ZVT Boost Converter.

Mode 1. (t_0, t_1):

At t_0, the auxiliary switch S_a is turned on and starts a resonance process between $i_{Lr1}(t)$ and $v_{Cr}(t)$. At the same time $i_{Lr2}(t)$ begins to increase linearly until it reaches the input current value. The voltage and current expressions to this mode are given by:

$$v_{Cr}(t) = V_0 + (V_{Cr}(t_0) - V_0)\cos(\omega_1 .t) + Z_1 .I_{Lr1}(t_0) sin(\omega_1 .t) \tag{1}$$

$$i_{Lr1}(t) = \frac{V_0}{Z_1} sin(\omega_1 t) + I_{Lr1}(t_0)\cos(\omega_1 t) \tag{2}$$

$$v_{Cs}(t) = V_0 \tag{3}$$

$$i_{Lr2}(t) = \frac{V_0}{L_{r2}} t \tag{4}$$

The time interval of this mode is given by:

$$\Delta t_1 = t_1 - t_0 = \frac{I_i L_{r2}}{V_0} \tag{5}$$

Where the impedance Z_1 is given by

$$Z_1 = \sqrt{\frac{L_{r1}}{C_r}} \tag{6}$$

And the resonant frequency ω_1 by:

$$\omega_1 = \frac{1}{\sqrt{L_{r1} C_r}} \tag{7}$$

Mode 2. (t_1, t_2):

When the current through L_{r2} is equal to I_i, boost diode D turns off. Hence, other resonant process begins between $i_{Lr2}(t)$ current and $v_{Cs}(t)$ voltage. This process will completely discharge the energy stored into C_s. This mode lasts until the voltage $v_{Cs}(t)$ reaches zero and the current through the auxiliary switch also reaches zero. The voltage and current behavior are given by the expressions:

$$v_{Cr}(t) = V_0 + (V_{Cr}(t_1) - V_0)\cos(\omega_1 t) + Z_1 I_{Lr1}(t_1) sin(\omega_1 t) \quad (8)$$

$$i_{Lr1}(t) = \frac{(V_0 - V_{Cr}(t_1))}{Z_1} sin(\omega_1 t) + I_{Lr1}(t_1)\cos(\omega_1 t) \quad (9)$$

$$v_{Cs}(t) = V_0 \cos(\omega_2 t) \quad (10)$$

$$i_{Lr2}(t) = I_i + \frac{V_0}{Z_2} sin(\omega_2 t) \quad (11)$$

The time of this mode is given by:

$$\Delta t_2 = t_2 - t_1 = \frac{\pi + sin^{-1}\left(\frac{1}{k_2}\right)}{\omega_1} - \frac{\frac{I_i Z_2}{V_0}}{\omega_2} \quad (12)$$

Where the impedance Z_2 is given by (13) and the resonant frequency ω_2 by (14):

$$Z_2 = \sqrt{\frac{L_{r2}}{C_s}} \quad (13)$$

$$\omega_2 = \frac{1}{\sqrt{L_{r2} C_s}} \quad (14)$$

And, the factor k_2 defines the relation between the maximum current through the resonant inductors.

$$k_2 = \frac{I_{Lr1(\max)}}{I_{Lr2(\max)}} \quad (15)$$

Mode 3. (t_2, t_3):

At instant t_2, the current through the inductor L_{r2} reaches its highest value, given by:

$$I_{Lr2(\max)} = I_i + \Delta I \quad (16)$$

Where the amount of current that exceeds the input current, defined as ΔI, is given by:

$$\Delta I = \frac{V_0}{Z_2} \quad (17)$$

During this mode, both switch anti-parallel diode D_1 and D_a turn on. To achieve soft commutation conditions for the main switch turn-on and for the auxiliary switch turn-off, their gate-drain signals must be turned on and off, respectively during this circuit mode. The voltage and current expressions to this mode are given by:

$$v_{Cr}(t) = V_0 + (V_{Cr}(t_2) - V_0)\cos(\omega_1 t) + Z_1 I_{Lr1}(t_2) sin(\omega_1 t) \quad (18)$$

$$i_{Lr1}(t) = \frac{(V_0 - V_{Cr}(t_2))}{Z_1} sin(\omega_1 t) + I_{Lr1}(t_2)\cos(\omega_1 t) \quad (19)$$

$$v_{Cs}(t) = 0 \quad (20)$$

$$i_{Lr2}(t) = I_{Lr2}(t_2) \quad (21)$$

The time of this mode is given by:

$$\Delta t_3 = t_3 - t_2 = \frac{\pi - 2sin^{-1}\left(\frac{1}{k_2}\right)}{\omega_1} \quad (22)$$

Mode 4. (t_3, t_4):

At t_3, the diode D_a turns off and the current $i_{Lr2}(t)$ decreases in a resonant way through L_{r1}, L_{r2} and C_r. This mode ends when $v_{Cr}(t)$ reaches zero and the diode D_b turns on. The voltage and current expressions to this mode are given by:

$$v_{Cr}(t) = V_0 + \left(V_{Cr}(t_3) - V_0\right)\cos(\omega_3 t) + I_{Lr1}(t_3).sin(\omega_3 t) \quad (23)$$

$$i_{Lr1}(t) = \frac{\left(V_{Cr}(t_3) - V_0\right)}{Z_3}.sin(\omega_3 t) + I_{Lr1}(t_3).\cos(\omega_3 t) \quad (24)$$

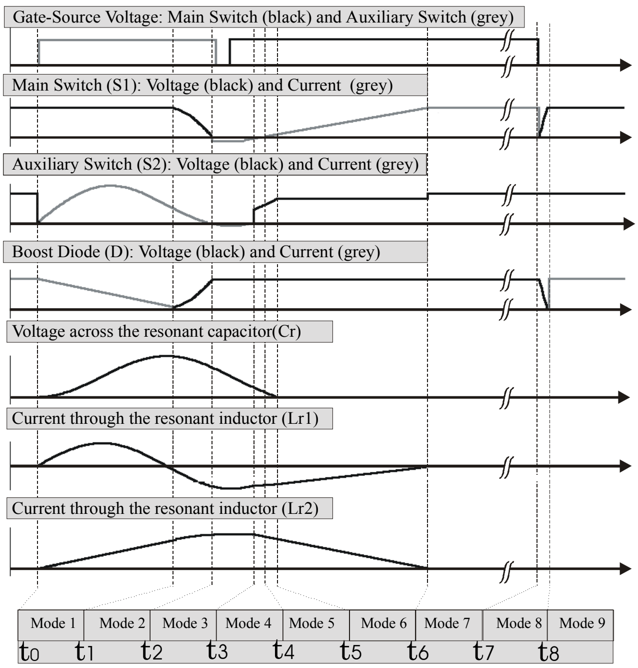

Fig. 4 – Main theoretical waveforms.

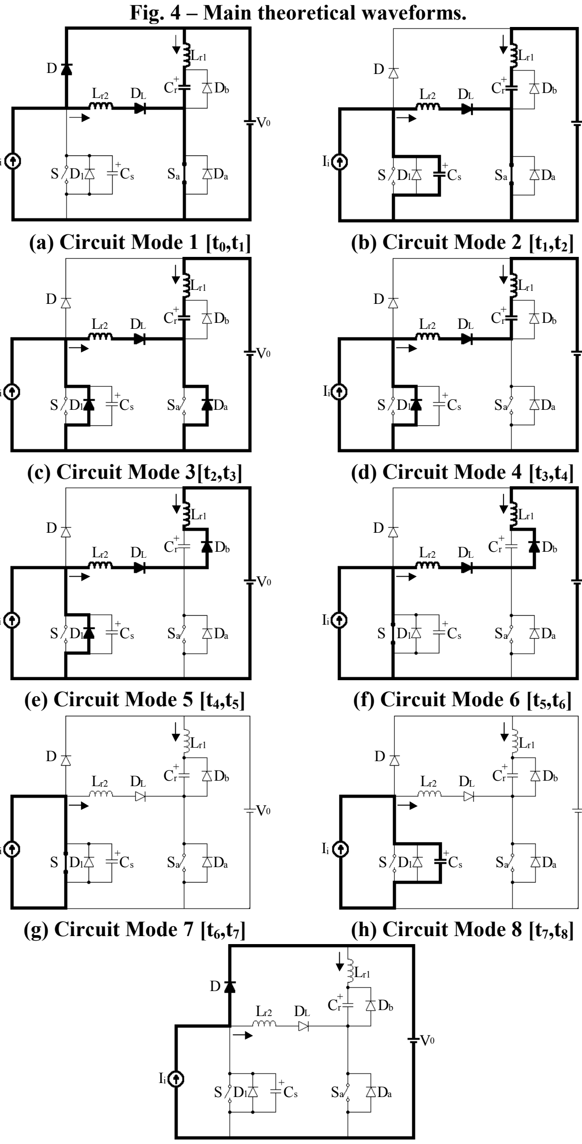

(a) Circuit Mode 1 [t_0,t_1] **(b) Circuit Mode 2 [t_1,t_2]**

(c) Circuit Mode 3[t_2,t_3] **(d) Circuit Mode 4 [t_3,t_4]**

(e) Circuit Mode 5 [t_4,t_5] **(f) Circuit Mode 6 [t_5,t_6]**

(g) Circuit Mode 7 [t_6,t_7] **(h) Circuit Mode 8 [t_7,t_8]**

(i) Circuit Mode 9 [t_8,t_9]

Fig. 5 – Circuit Modes during one switching period.

$$v_{Cs}(t) = 0 \quad (25)$$

$$i_{Lr2}(t) = -i_{Lr1}(t) \quad (26)$$

The time of this mode is given by:

$$\Delta t_4 = t_4 - t_3 = \frac{tg^{-1}\left[\dfrac{-v_{Cr}(t_3)}{V_0 + Z_3.I_{Lr1}(t_3)}\right]}{\omega_3} \quad (27)$$

Where the impedance Z_3 is given by:

$$Z_3 = \sqrt{\frac{L_{r1} + L_{r2}}{C_r}} \quad (28)$$

And the resonant frequency ω_3 by:

$$\omega_3 = \frac{1}{\sqrt{(L_{r1} + L_{r2})C_r}} \quad (29)$$

Mode 5. (t_4, t_5):

At t_4, the current $i_{Lr2}(t)$ decreases linearly until it reaches I_i, when D_1 is turned off. The voltage and current expressions to this mode are given by:

$$v_{Cr}(t) = 0 \quad (30)$$

$$i_{Lr1}(t) = \frac{V_0}{L_{r1} + L_{r2}}.t + I_{Lr1}(t_4) \quad (31)$$

$$v_{Cs}(t) = 0 \quad (32)$$

$$i_{Lr2}(t) = -i_{Lr1}(t) \quad (33)$$

The time of this mode is given by:

Mode 6. (t_5, t_6):

The current $i_{Lr2}(t)$ continues to ramp down until it reaches zero and the current through main switch S reaches I_i. In this mode, the expressions to the voltages and currents are the same as in the mode 5. The time of this mode is given by:

$$\Delta t_6 = t_6 - t_5 = \frac{I_{Lr1}(t_5).(L_{r1} + L_{r2})}{V_0} \quad (35)$$

Mode 7. (t_6, t_7):

The operation of the circuit at this mode is similar to its hard-switching counterpart. The input current flows through the main switch S. The time of this mode is given by the duty-cycle of the PWM modulation.

Mode 8. (t_7, t_8):

At t_7, the main switch S is turned off and the current I_i is diverted to the capacitor C_s and its voltage is linearly charged up to output converter voltage V_0. The voltage and current expressions to this mode are given by:

$$v_{Cr}(t) = 0 \quad (36)$$

$$i_{Lr1}(t) = 0 \quad (37)$$

$$v_{Cs}(t) = \frac{I_i}{C_s}.t \quad (38)$$

$$i_{Lr2}(t) = 0 \quad (39)$$

The time of this mode is given by:

$$\Delta t_8 = t_8 - t_7 = \frac{C_s.V_0}{I_i} \quad (40)$$

Mode 9. (t_8, t_9):

When $v_{Cs}(t)$ voltage reaches V_0, the boost diode D turns on, begins another switching cycle.

III. SOFT COMMUTATION CONDITIONS

- **Main switch turn-off (ZVS)**

As described in Section II, mode 8, after main switch S to be turned off, the input current is diverted from switch to a snubber capacitor C_S. As a result, voltage across the main switch increases with controlled *dv/dt* achieving zero voltage turn-off. The capacitance value is given by expression (41) as follows:

$$C_s = \frac{I_i\, t_f}{2k_s V_0} \quad (41)$$

Where t_f is function of the semiconductor device used and factor k_s is chosen to reduce the commutation energy. The range of k_s is defined in (42):

$$0 < k_s < 1 \quad (42)$$

- **Main switch turn-on (ZVS)**

To achieve main switch turn-on with zero voltage, initially is necessary to divert the input current from boost diode D to inductance L_{r2} and after, to discharge completely the snubber capacitor C_s. This way the resonant process between $i_{Lr2}(t)$ and $v_{Cs}(t)$ must lasts until $v_{Cs}(t)$ achieves zero. This condition is assured by the following expression:

$$\omega_1 = \frac{2k_1\omega_2}{(2 + k_1\pi)}\left(\pi + sin^{-1}\left(\frac{1}{k_2}\right)\right) \quad (43)$$

- **Auxiliary switch turn-on (ZCS)**

As described in Section II, modes 1 and 2, by the presence of inductors L_{r1} and L_{r2} current through auxiliary switch S_a increases with controlled *di/dt* achieving zero current turn-on. Furthermore, by an adequate choice of L_{r2}, the reverse-recovery losses of boost diode D could be minimized. The expression (44) can be used to choose the inductance L_{r2}:

$$L_{r2} > \frac{V_0}{\left(\dfrac{d}{dt} i_D\right)} \quad (44)$$

- **Auxiliary switch turn-off (ZCS)**

To achieve zero current turn-off of the auxiliary switch S_a, the following restrictions must be satisfied:

i. The relation between the maximum values of current through each one of the resonant inductors L_{r1} and L_{r2} given by expression (15) must be defined as follows:

$$k_2 > 1 \quad (45)$$

This way, the characteristic impedance of the resonant tank Z_1 is given by:

$$Z_1 = \frac{V_0}{I_i k_2 (1 + k_1)} \quad (46)$$

ii. To assure that the maximum value of current through L_{r2} occurs before $i_{Lr1}(t)$ achieves its maximum negative value, the relation between the resonant frequencies ω_1 and ω_2, given by (43) also must be assured.

IV. DESIGN GUIDELINES

In this section, a design procedure and an example of how to determine the component values of the proposed improved ZVT PWM boost converter is given.

The input data are defined as follows:

Output Power	$P_0 = 1000\ W$
Output Voltage	$V_0 = 400\ V$
Input Voltage	$V_i = 150\ V\ (\pm\ 10\%)$
Operation Frequency	$f_s = 100\ kHz$
Approximate efficiency	$\eta \geq 95\ \%$

The design guidelines is composed by twelve steps described as follows:

a) The value of the capacitance C_s can be determined by a turn-off capacitive snubber procedure [16]. However, in order to minimize the number of auxiliary components, in this example, C_s is adopted as the intrinsic output capacitance of the semiconductor device (MOSFET – IRP450). Thus, C_s is defined as:

$$C_s = 0.4\,nF \tag{47}$$

b) From the output power and the approximate efficiency, the input power is defined:

$$P_i = \frac{P_0}{\eta} = 1050\ W \tag{48}$$

c) From the input power and the input voltage, the input current is defined by:

$$I_i = \frac{P_i}{V_i} = 7.0\,A \tag{49}$$

d) The inductance L_{r2} is obtained from the expression (50) where the factor k_1 is defined by (51) and was chosen as equal to $k_1 = 0.23$.

$$L_{r2} = \frac{C_s}{k_1^{\ 2}}\left(\frac{V_0}{I_i}\right)^2 = 27.1\,\mu H \tag{50}$$

$$k_1 = \frac{\Delta I}{I_i} \tag{51}$$

e) The impedance Z_2 is calculated by:

$$Z_2 = \sqrt{\frac{L_{r2}}{C_s}} = 278.26\,\Omega \tag{52}$$

f) The resonant frequency ω_2 is calculated by:

$$\omega_2 = \frac{1}{\sqrt{L_{r2}C_s}} = 10.27\ M\ rad/s \tag{53}$$

g) To assures ZCS commutation to switch S_a, k_2 is defined by (45) and was chosen as follows:

$$k_2 = 1.1 \tag{54}$$

h) Substituting k_2 and k_1 values in expression (46), the impedance Z_1 is given by:

$$Z_1 = 47.299\,\Omega \tag{55}$$

i) By the expression (43), ω_1 is:

$$\omega_1 = 7.431 M\ rad/s \tag{56}$$

j) The inductance of the resonant tank is given by:

$$L_{r1} = \frac{Z_1}{\omega_1} = 6.365\,\mu H \tag{57}$$

k) The capacitance of the resonant tank is given by:

$$C_r = \frac{1}{Z_1\omega_1} = 2.845\,nF \tag{58}$$

l) To minimize the maximum current through inductor L_{r2} at the instant t_2, the resonant frequencies ratio was chosen as follows:

$$\frac{\omega_2}{\omega_1} = 0.933 \tag{59}$$

This way, the inductance and capacitance values of the resonant tank are:

$$L_{r1} = 5.0\,\mu H \tag{60}$$

$$C_r = 1.65nF \tag{61}$$

V. Experimental Results

Following the design example shown in section IV, a 100 kHz, 1 kW improved ZVT PWM boost converter prototype has been implemented to verify the operation and the performance of the proposed improved ZVT commutation cell. The power circuit is shown in Fig. 9. Its main parameters are summarized in Table I. The main switch used was IRFP450 (MOSFET) and the auxiliary switch used was HGTP7N60C3D (600 V, 7 A) UFS (Ultra Fast Switches) series IGBT from Intersil Semiconductors, which present an anti-parallel hyperfast diode built-in.

The dashed lines in the power stage circuit diagram represent the clamped circuits used to limit the voltage spikes across switch S_a and diode D_L.

As can be seen in Fig. 10(a), the gate-source signal of switch S, is applied only after the voltage v_{DS} reaches zero, characterizing the zero voltage turn-on. To assure ZCS turn-off at auxiliary switch, its gate-source signal is removed after the current through it reaches zero, as shown in Fig. 10(b). Fig. 10(c) shows the voltage across the resonant capacitor C_r and the current through resonant inductor L_{r1} and L_{r2} currents.

Figure 11 shows the measured efficiency of the boost converter with the improved ZVT commutation cell as

Table 1
Experimental Parameters

Component	Parameter
***V_i* (input voltage)**	150 V
***V_0* (output voltage)**	400 V
***P_0* (output power)**	1.0 kW
***f_s* (switching frequency)**	100 kHz
***L* (input filter)**	0.90 mH
***C* (output filter)**	150 uF
***S* (main switch)**	IRFP450
***S_a* (auxiliary switch)**	HGTP7N60C3D
***D* (boost diode)**	MUR1560
***D_L* (blocking diode)**	MUR1560
***D_b* (auxiliary diode)**	RHRP8120
***L_{r1}* (resonant inductor)**	5.0 µH
***L_{r2}* (resonant inductor)**	27.1 µH
***C_s* (resonant capacitor)**	400 pF ($C_s = C_{oss}$)
***C_r* (resonant capacitor)**	1.65 nF (= 2 x 3.3 nF)

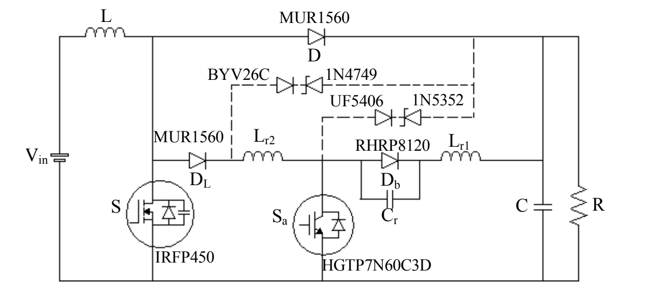

Fig. 9– Power stage circuit diagram of the ZVT boost converter.

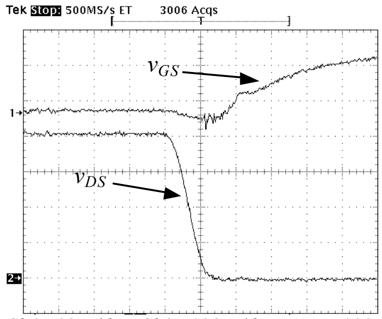

Grid: *Ch1=10 V/div, Ch2=100 V/div, Time=100 ns/div.*

(a) Main Switch: *Ch1 – $v_{GS}(t)$, Ch2 – $v_{DS}(t)$.*

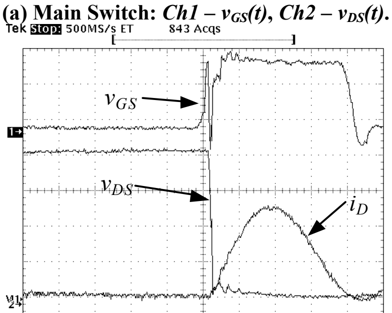

Grid: *Ch1=10 V/div, Ch2=100 V/div, Ch3= 4 A/div, Time=100 ns/div.*

(b) Auxiliary Switch: *Ch1 – $v_{GS}(t)$, Ch2 – $v_{DS}(t)$,Ch3 – $i_D(t)$.*

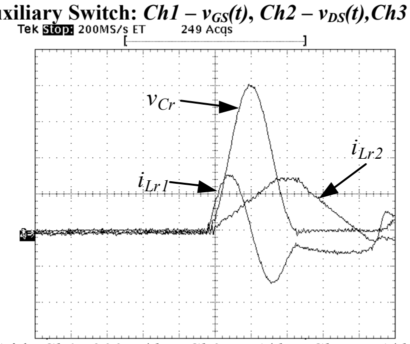

Grid: *Ch1=200 V/div, Ch3=5 A/div, Ch4=5 A/div.*

(c) Resonant Elements: *Ch1 $v_{Cr}(t)$, Ch3 – $i_{Lr2}(t)$, Ch4 - $i_{Lr1}(t)$, Time=250 ns/div*

Fig.10 – Experimental results.

function of the output power, whose value was equal to 95.2% at full load (1 kW). Fig. 11 also includes the efficiency curve of the same circuit without the proposed commutation cell for comparison proposes. Without the proposed commutation cell the converter efficiency at full load was 94.4%.

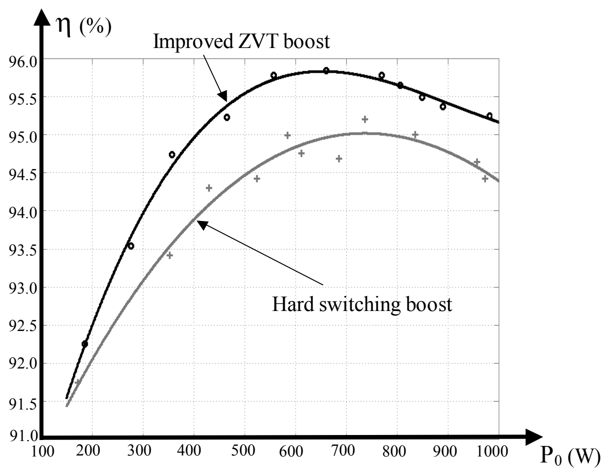

Fig. 11 – Converters efficiencies.

VI. CONCLUSIONS

A family of Improved ZVT PWM converters is presented. These converters present the merits of [1] and furthermore, achieve soft switching at zero current (ZCS) for auxiliary switch. To obtain these characteristics a resonant tank is used as auxiliary commutation source to control the current through the auxiliary switch.

Operating principles and commutation process were described and verified by experimental results, which were obtained from a prototype of 1 kW operating at 100 kHz and presented efficiency gain of 0.5 % compared with its PWM counterpart at full load.

ACKNOWLEDGMENT

The authors would like to express their special thanks to Thornton Inpec Eletrônica Ltda and Siemens-Icotron of Brazil for material support.

REFERENCES

[1] G. Hua, C.-S. Leu, F. C. Y. Lee, "Novel Zero-Voltage-Transition PWM Converters", in *IEEE Power Electronics Specialists Conference*, 1992, pp. 55-60;

[2] R. Streit, D. Tollik, "A High Efficiency Telecom Rectifier Using A Novel Soft-Switched Boost-Based Input Current Shaper", in *INTELEC*, 1991, pp. 720-726;

[3] P. J. M. Menegás, M. A. Có, D. S. L. Simonetti, J. L. F. Vieira, "Improving the Operation of ZVT DC-DC Converters", in *IEEE Power Electronics Specialists Conference*, 1999;

[4] G. Moschopoulos, P. Jain, G. Joos, "A Novel Zero-Voltage Switched PWM Boost Converter", in *IEEE Power Electronics Specialists Conference*, 1995;

[5] C.-J. Tseng, C.-L. Chen, "Novel ZVT-PWM Converters With Active Snubbers", in *IEEE Transactions on Power Electronics*, 1998, Vol. 13, n. 5, pp. 861-869;

[6] K. M. Smith, K. M. Smedley, "A Comparison of Voltage-Mode Soft-Switching methods for PWM Converters", in *IEEE Transactions on Power Electronics*, 1997, Vol. 12, n. 2, pp. 376-386;

[7] G. Moschopoulos, P. Jain, G. Joos, Y.-F. Liu, "A Zero-Voltage Switched PWM Boost Converter With An Energy Feedforward Auxiliary Circuit", in *IEEE Power Electronics Specialists Conference*, 1996;

[8] D. M. Xu, J. M. Zhang, Y. C. Ren, Z. Qian, "A Novel Single-Phase Active-Clamped ZVT-PWM PFC Converter", in *IEEE Applied Power Electronics Conference*, 2000;

[9] L. Yang, C. Q. Lee, "Analysis and Design of Boost Zero-Voltage-Transition PWM Converter", in *IEEE Applied Power Electronics Conference*, 1993, pp. 707-713;

[10] N. P. Filho, V. J. Farias, L. C. de Freitas, "A Novel Family of DC-DC PWM Converters Using the Self-Resonance Principle", in *IEEE Power Electronics Specialists Conference*, 1994, pp. 1385-1391;

[11] F. C. Y. Lee, "High-Frequency Quasi-Resonant Converter Topologies", in *Proceedings of the IEEE*, 1988, Vol. 76, n. 4, pp. 377-390;

[12] C. P. Henze, H. C. Martin, D. W. Parsley, "Zero-Voltage-switching in High Frequency Power Converters Using Pulse Width Modulation", in *IEEE Applied Power Electronics Conf.*, 1988, pp. 33-40;

[13] D. C. Martins, F. J. DE Seixas, I. Barbi, J. A. Brilhante, "A Family of DC-to-DC PWM Converters Using a New ZVS Commutation Cell", in *IEEE Power Electronics Specialists Conference*, 1993, pp. 524-530;

[14] H. Irie, "Resonant Switches in Common Equivalent Circuit of DC/DC Converters", *IPEC*,1991, pp. 362-368

[15] N. Mohan, T. M. Undeland and W. P. Robbins, "Power Electronics - Converters, Applications and Design", John Wiley & Sons, NY, 1995.